Online Supplement for
The Rack Orientation and Curvature Problem for Retailers

Bradley Guthrie and Pratik J. Parikh

Appendix A. Models for Space and Aspect Ratio

We estimate the floor space a of a given layout by the rectangular area that bounds the perimeter of the layout. Let Le and Wi be the length and width of this rectangular bounded area. To find Le and Wi, we must determine the coordinates of the edges for this rectangle along the width (x-direction) and the length (y-direction). Let these be represented as (x^{min}, x^{max}), and (y^{min}, y^{max}), respectively, such that $Wi = x^{max} - x^{min}$ and $Le = y^{max} - y^{min}$. We first, however, must derive x_{nf}^{min}, x_{nf}^{max}, y_{nf}^{min}, and y_{nf}^{max}, which are the edge coordinates for each face f on rack n. Further, let x_{nf}^{mid} and y_{nf}^{mid} be the coordinates of the center of curvature for face f on rack n; r_f notates the radius for face f. Depending on the combination of θ and α for a specific layout, these extreme points may fall on faces F2, F3, or F4 (i.e., outer face or either endcap). We propose an exact procedure to determine Le and Wi, as illustrated in Figure A1, which help in estimating the floor space ($a = Le \times Wi$) and the aspect ratio ($r = \frac{Le}{Wi}$). Figure A2 subsequently illustrates three example layouts with their respective dimensions (Le, Wi) and locations of values x^{max}, x^{min}, y^{max}, and y^{min}.

(1) **For** $n = 1$ or $n = N$

(2) **For** $f \in$ {F2, F3, F4}

(3) **Compute** extreme points of face f in x and y directions

(4) $x_{nf}^{max} = x_{nf}^{mid} + r_f$

(5) $x_{nf}^{min} = x_{nf}^{mid} - r_f$

(6) $y_{nf}^{max} = y_{nf}^{mid} + r_f$

(7) $y_{nf}^{min} = y_{nf}^{mid} - r_f$

(8) **Determine** if points fall on the physical part of rack (per Table 2).

(9) **Compare** the feasible extreme points to determine x^{max}, x^{min}, y^{max}, and y^{min}

(10) $x^{max} = \max\{x_{nf}^{max}\ \forall f, n\}$, $x^{min} = \min\{x_{nf}^{min}\ \forall f, n\}$

(11) $y^{max} = \max\{y_{nf}^{max}\ \forall f, n\}$, $y^{min} = \min\{y_{nf}^{min}\ \forall f, n\}$

(12) **Compute** $\boldsymbol{Le} = y^{max} - y^{min}$ and $\boldsymbol{Wi} = x^{max} - x^{min}$

Figure A1. Exact procedure to estimate ***Le*** and ***Wi*** of the layout

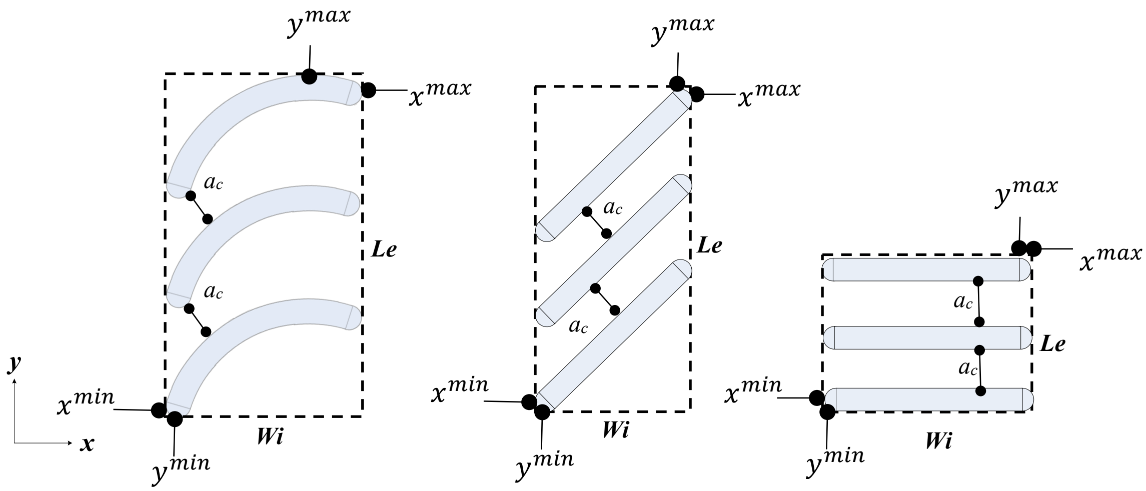

(a) $\theta = 60°$, $\alpha = 90°$ (b) $\theta = 45°$, $\alpha = 0°$ (c) $\theta = 90°$, $\alpha = 0°$

Figure A2. Dimensions of *Le* and *Wi* for example layouts with $N = 3$

Using the above procedure, we can compute the floor space for any combination of θ and α. Figure A3 presents the floor space (right side of the layout only, both sides are identical) for 133 combinations of θ and α with values of θ ranging from 0° to 180° in steps of 10° and values of α ranging from 0° to 180° in steps of 30°. Design parameters are identical to those in Table 5. For this specific configuration, the values of θ that provide maximum floor space are in the ranges (θ=40°, θ=50°) and (θ=130°, θ=140°); this is consistent for all values of α. Minimum floor space meanwhile occurs at both θ=0° and θ=180° (again, for all values of α). The value of α however that maximizes floor space *changes* with respect to θ. When *θ=0°, 90°,* and *180°, α=150°* provides maximum floor space; when θ=40° or 140°*,* α=90° provides maximum floor space. A curvature of α=0° meanwhile results in the minimum floor space for all values of θ. While it would seem intuitive that space would always increase as α increases from 0° to 180°, because our layouts maintain a fixed shelf-area for any value of α, the chord length (i.e., aisle length) rapidly decreases as α approaches 180°. This reduces *Wi*, thereby, lowering the total floor space.

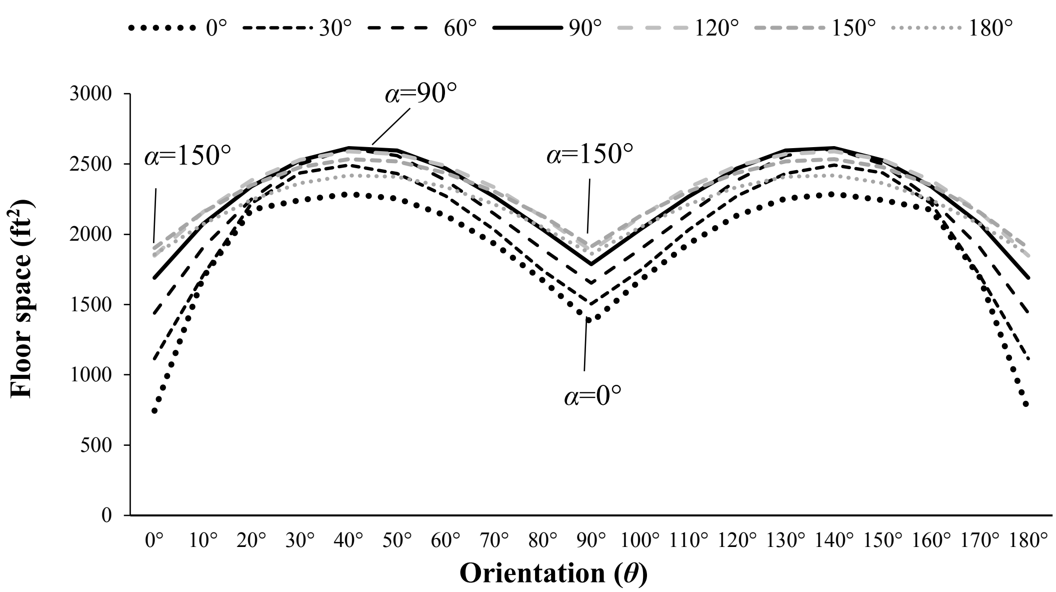

Figure A3. Change in floor space (ft^2) for various rack orientations and curvatures

Aspect ratio (r) is illustrated in Figure A4. While θ=0° and θ =180° (both at α=0°) required the lowest space, they both resulted in a long and skinny section; r=29.77. The rack layout of θ=90° and α=0° meanwhile resulted in layouts that were short and wide; r=0.7. Notice here for θ values 0° and 10° (alternately, 180° and 170°) the aspect ratio *decreases* as α increases to 180°. This trend, however, steadily shifts to *increasing* for an increasing α as θ approaches 90°. This phenomenon occurs because of the nature of curved racks; increase either *Wi* or *Le* values relative to α=0°. That is, for θ values closer to 0° or 180°, the curved racks cause an increase in *Wi*, thereby lowering the aspect ratio (as *Le* is much higher). In contrast, for θ values closer to 90°, the curved racks cause *Le* to increase, subsequently increasing the aspect ratio (as *Wi* is much higher in this case).

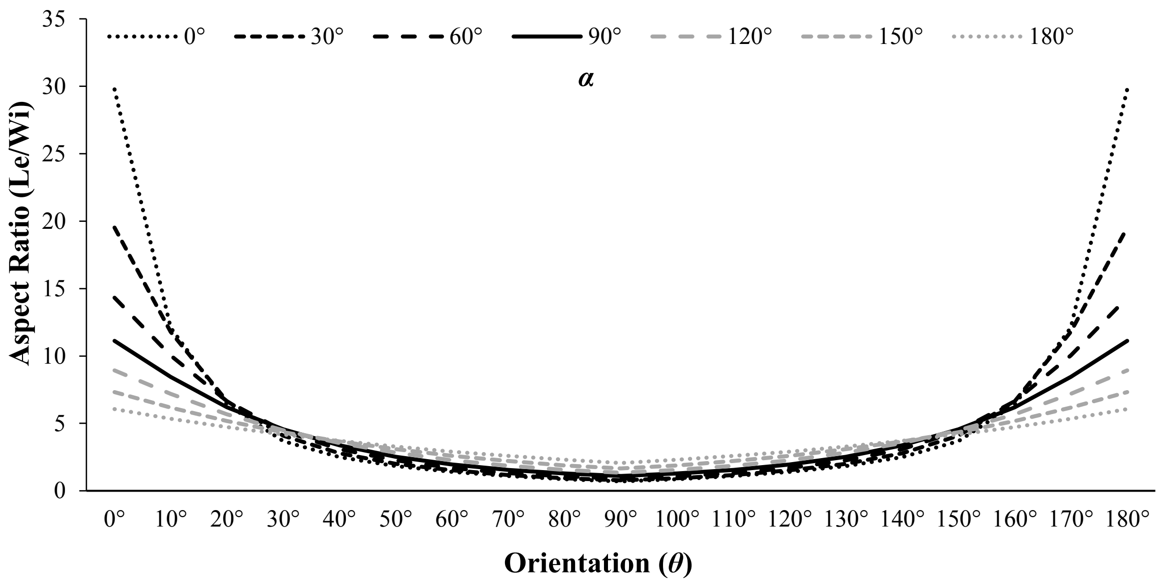

Figure A4. Change in Aspect Ratio with varying values of θ and α

Appendix B. Example for Deriving v_{ly}

To describe our procedure for deriving v_{ly} (i.e., the probability that a shopper's focal point will fall on location l at step y), we present step-by-step mathematical expressions considering a single step y and a single location l; see Figure B1. From Section 3.2.2, this procedure is divided into 3 stages (i.e., i, ii, and iii). For (i), we first compute the angular coordinates (i.e., Ψ_{li}, Γ_{li}) from the shopper to each vertex i of each location l. Figure B2 (from Section 3.2.2) details all the coordinates and angles we use to derive these coordinates.

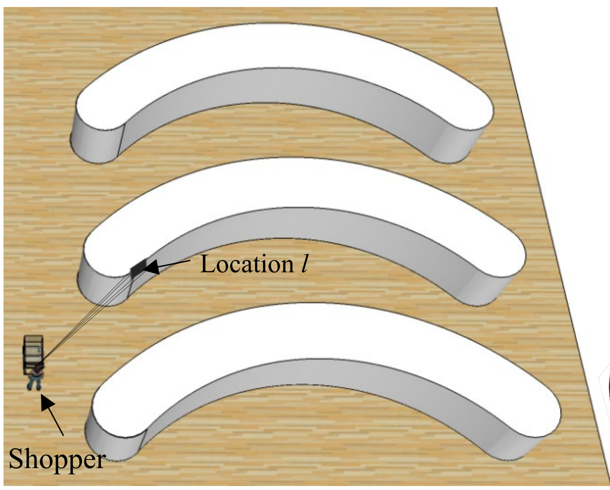

Figure B1. View of shopper and location l

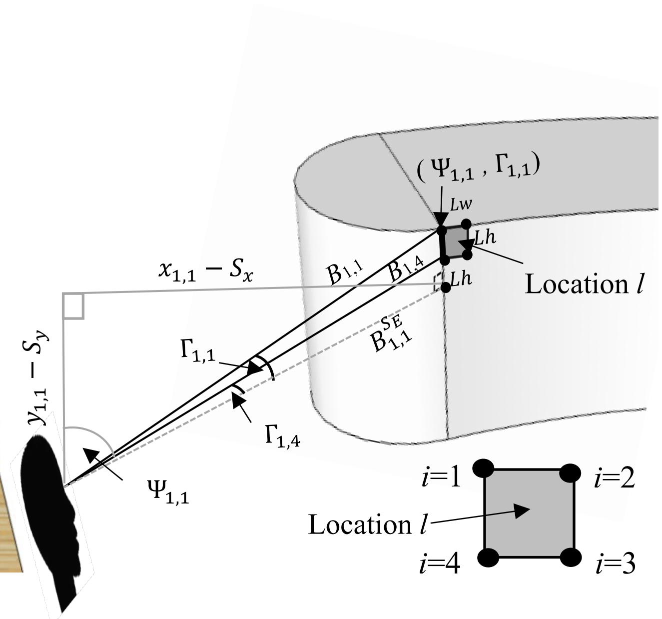

Figure B2. Determining angular coordinates of location l

The following are values corresponding to position y of shopper and location l (with 1-4 as indices for each vertex):

S_E = 5 ft, S_x = 0 ft, S_y = 65 ft, $z_{1,1}$ = 7 ft, $z_{1,2}$ = 7 ft, $z_{1,3}$ = 6 ft, $z_{1,4}$ = 6 ft, Lh = 1 ft

$x_{1,1}$= 6.77 ft, $y_{1,1}$=74.42 ft, $x_{1,4}$= 6.77 ft, $y_{1,4}$=74.42 ft, $x_{1,2}$= 7.53 ft, $y_{1,2}$=75.15 ft, $x_{1,3}$= 7.53 ft, $y_{1,3}$= 75.15 ft

Using these, we can determine the unknown distances and angles from the shopper to each vertex of location l using equations presented in Section 3.2.2:

$$B_{li}^{S_E} = \sqrt{\left(y_{li} - S_y\right)^2 + (x_{li} - S_x)^2}; \text{ i.e., } B_{1,1}^{S_E} = \sqrt{(74.42 - 65)^2 + (6.77 - 0)^2} = 11.60 \text{ ft}$$

$$B_{li} = \sqrt{\left(B_{li}^{S_E}\right)^2 + (|z_{li} - S_E| * Lh)^2}; \text{ i.e., } B_{1,1} = \sqrt{(11.60)^2 + (|7 - 5| * 1)^2} = 11.77 \text{ ft}$$

$$\Psi_{li} = \sin^{-1}\left(\frac{x_{li} - S_x}{B_{li}^{S_E}}\right); \text{ i.e., } \Psi_{1,1} = \sin^{-1}\left(\frac{6.77 - 0}{11.60}\right) = 35.69°$$

$$\Gamma_{li} = \sin^{-1}\left(\frac{|z_{li} - S_E| * Lh}{B_{li}}\right); \text{ i.e., } \Gamma_{1,1} = \sin^{-1}\left(\frac{|7 - 5| * 1}{11.77}\right) = 9.78°$$

Similarly, using the above equations we can also find:

$B^{S_E}_{1,2}$ = 12.64 ft	$B^{S_E}_{1,3}$ = 12.64 ft	$B^{S_E}_{1,4}$ = 11.60 ft
$B_{1,2}$ = 12.79 ft	$B_{1,3}$ = 12.68 ft	$B_{1,4}$ = 11.64 ft
$\Psi_{1,2}$ = 36.57°	$\Psi_{1,3}$ = 36.57°	$\Psi_{1,4}$ = 35.69°
$\Gamma_{1,2}$ = 8.99°	$\Gamma_{1,3}$ = 4.52°	$\Gamma_{1,4}$ = 4.93°

For (ii), recall from Section 3.2.2 that the second step to compute v_{ly} is to generate the probability distribution for shopper focal point position (i.e., Ξ_{Ω_H,Ω_V}). Table B1 provides an outline of the data we collected from 18 participants. For each participant, and at time steps of 0.016 seconds (at 60 Hz sampling rate), we recorded the horizontal (Ω_H) and vertical (Ω_V) angles of their head position.

Table B1. Outline of participant data

Participant	Time (s)	Ω_H	Ω_v
1	0	1.34	4.32
1	0.016	2.56	3.44
…	…	…	…

We then computed the frequency of Ω_H and Ω_V that fell in intervals of $\zeta_H = \zeta_V$ =0.25° (i.e., F_{Ω_H,Ω_V}); for this example, we use intervals of $\zeta_H = \zeta_V$ =1°. Figure B3 shows F_{Ω_H,Ω_V} for ranges near the values of Ψ_{li} and Γ_{li} for location 1 in this example. Figure B4 meanwhile shows the result of our smoothing process, which accounts for eye-movement of 15° surrounding each bin. Finally, we compute the probability of a shopper's focal point falling within each interval as $p(\Xi_{\Omega_H,\Omega_V}) = \frac{F_{\Omega_H,\Omega_V}}{\sum F_{\Omega_H,\Omega_V}}$; see Figure B5.

	F_{Ω_H,Ω_V}	Ω_H 34°	35°	36°	37°	38°
Ω_V	10°	0	1	0	0	0
	9°	4	3	3	2	1
	8°	1	3	1	4	5
	7°	2	3	1	2	0
	6°	4	2	2	0	4
	5°	2	6	7	8	8
	4°	9	14	18	15	10

Figure B3. Raw data, F_{Ω_H,Ω_V}

	F_{Ω_H,Ω_V}	Ω_H 34°	35°	36°	37°	38°
Ω_V	10°	2	2	2	2	2
	9°	3	3	3	3	3
	8°	4	4	4	4	4
	7°	5	5	5	5	5
	6°	7	7	7	7	7
	5°	10	10	10	9	9
	4°	12	12	12	12	11

Figure B4. Smooth data with eye movement

	Ξ_{Ω_H,Ω_V}	Ω_H 34°	35°	36°	37°	38°
Ω_V	10°	0.005%	0.006%	0.006%	0.006%	0.006%
	9°	0.007%	0.008%	0.008%	0.008%	0.008%
	8°	0.010%	0.011%	0.011%	0.011%	0.011%
	7°	0.015%	0.015%	0.015%	0.015%	0.015%
	6°	0.020%	0.020%	0.021%	0.021%	0.020%
	5°	0.027%	0.027%	0.027%	0.027%	0.026%
	4°	0.033%	0.033%	0.033%	0.032%	0.032%

Figure B5. Probability mass function of shopper's eye fixation, Ξ_{Ω_H,Ω_V}

The final step (iii) for deriving v_{ly} is to sum all of the intervals in Ξ_{Ω_H,Ω_V} that fall over the effective area of location l. Figure B6 illustrates this process by showing the effective area of location l broken down in a grid with intervals of $\zeta = 1°$ as used in deriving Ξ_{Ω_H,Ω_V} (see Figure B5). We find these intervals by first computing the outer limits of both vertical and horizontal angles (i.e., Ψ_{li} and Γ_{li}) to the vertices i of location l. For the location l shown in Figure B6, we estimate these outer limits as follows:

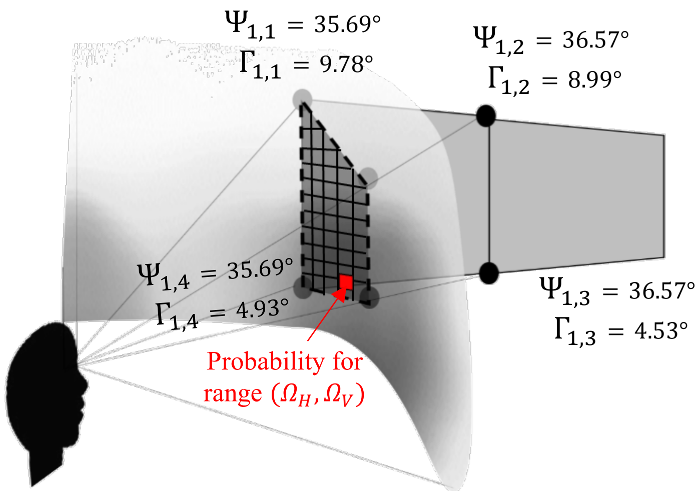

Figure B6. Overlapping of Ξ_{Ω_H,Ω_V} over location l

$\zeta_H \left\lfloor \frac{\min\{\Psi_{1,1},\Psi_{1,4}\}}{\zeta_H} \right\rfloor \leq \Omega_H \leq \zeta_H \left\lceil \frac{\max\{\Psi_{1,2},\Psi_{1,3}\}}{\zeta_H} \right\rceil$ and $\zeta_V \left\lfloor \frac{\min\{\Gamma_{1,3},\Gamma_{1,4}\}}{\zeta_V} \right\rfloor \leq \Omega_V \leq \zeta_V \left\lceil \frac{\max\{\Gamma_{1,1},\Gamma_{1,2}\}}{\zeta_V} \right\rceil$; i.e.,

$1 \left\lfloor \frac{\min\{35.69°,35.69°\}}{1} \right\rfloor \leq \Omega_H \leq 1 \left\lceil \frac{\max\{36.57°,36.57°\}}{1} \right\rceil$ and $1 \left\lfloor \frac{\min\{4.53°,4.93°\}}{1} \right\rfloor \leq \Omega_V \leq 1 \left\lceil \frac{\max\{9.78°,8.99°\}}{1} \right\rceil$;

i.e., $35° \leq \Omega_H \leq 37°$ and $4° \leq \Omega_H \leq 9°$.

Following this, we then sum all intervals in Ξ_{Ω_H,Ω_V} that fall within both of the above two ranges. These ranges are surrounded by the dark border in Figure B7. Thus,

$v_{ly} = E_{ly} * \sum_{\Omega_H,\Omega_V}(\Xi_{\Omega_H,\Omega_V})$ for $35° \leq \Omega_H \leq 37°$ and $4° \leq \Omega_H \leq 9°$

$= 1 \times (0.00006 + 0.00006 + 0.00006 + 0.00008 + 0.00008 + 0.00008 + 0.00011 + 0.00011 + 0.00011 + 0.00015 + 0.00015 + 0.00015 + 0.00020 + 0.00021 + 0.00021 + 0.00027 + 0.00027 + 0.00027 + 0.00033 + 0.00033 + 0.00032)$

i.e., $v_{ly} =$ 0.00358

		Ω_H				
	Ξ_{Ω_H,Ω_V}	34°	35°	36°	37°	38°
Ω_V	10°	0.005%	0.006%	0.006%	0.006%	0.006%
	9°	0.007%	0.008%	0.008%	0.008%	0.008%
	8°	0.010%	0.011%	0.011%	0.011%	0.011%
	7°	0.015%	0.015%	0.015%	0.015%	0.015%
	6°	0.020%	0.020%	0.021%	0.021%	0.020%
	5°	0.027%	0.027%	0.027%	0.027%	0.026%
	4°	0.033%	0.033%	0.033%	0.032%	0.032%

Figure B7. Combinations of Ω_H and Ω_V that fall over location l

Appendix C. Product Category Assortment Data

Table C1 contains product data from a Midwest Retailer. Demand is in terms of units. Profits are categorized by category (i.e., low, medium high). Similarly, impulse rates are categorized by category; actual rates used in experiments are also shown. Allocated area is the derived allocated shelf space of that product category at the Midwest retailer, while 1ft x 1ft facings are the number of locations used in our experimental study. Further, our assigned aisle and side of the main aisle are given for each product category.

Table C1. Data from Midwest Retailer

Category	Product Category	Monthly Demand	Profit Category	Impulse Category	Impulse Rate	Allocated Area	1*1 Facings	Aisle	Side
1	Gravy Mix	6449	M	M	0.33	23.86	21	1	Right
2	Kraft Spreads	3644	M	M	0.29	20.08	14	1	Right
3	Italian Supplies	404	M	M	0.22	7.02	7	1	Right
4	Chili	8393	L	H	0.41	29.46	14	1	Right
5	Tuna	12379	L	M	0.30	37.94	35	1	Right
6	Pickles	5967	M	M	0.21	75.63	56	1	Right
7	Japanese Food	2698	L	M	0.24	41.82	42	1	Right
8	Croutons	2778	M	L	0.09	35.65	28	1	Right
9	Dressing	1823	L	M	0.17	23.70	7	1	Right
10	Condiments	10425	L	M	0.32	76.94	63	1	Right
11	Macaroni	11237	L	L	0.03	70.43	56	1	Right
12	Gatorade	5248	M	M	0.23	86.02	42	2	Right
13	Pizza Supplies	936	L	M	0.32	10.59	14	2	Right
14	Baking/Chocolate	4480	M	M	0.28	52.25	98	2	Right
15	Pasta Sauce	8821	L	M	0.30	73.26	84	2	Right
16	Jell-O	2775	L	M	0.27	25.42	14	2	Right
17	Canned Fruit	4607	L	H	0.47	27.66	21	2	Right
18	Tonic Water	7944	M	L	0.15	113.66	112	2	Right
19	Baking Supplies	946	L	M	0.32	10.76	7	2	Right
20	Rice	7519	M	L	0.07	58.67	56	2	Right
21	Oil	2158	L	L	0.08	24.56	7	2	Right
22	Seasonings	5267	M	L	0.04	25.67	21	2	Right
23	Seasonings/Spices	2145	L	L	0.07	5.22	7	2	Right
24	Brita Water	3291	M	L	0.03	25.34	14	2	Right
25	Beans	8456	L	M	0.31	40.83	35	2	Right
26	Canned Vegetables	14262	L	M	0.32	52.51	84	2	Right
27	Tomato Sauce	12676	L	L	0.08	18.87	14	2	Right
28	Sugar	3430	L	L	0.02	121.09	56	2	Right
29	Chocolate Syrup	1555	M	H	0.49	25.75	56	3	Right
30	Dried Fruit	2069	M	H	0.42	25.04	28	3	Right
31	Coffee	10344	L	M	0.25	104.36	126	3	Right
32	Peanut Butter	8931	M	L	0.15	54.21	56	3	Right
33	Health Bars	313	L	M	0.30	3.63	7	3	Right
34	Cereal	19257	L	M	0.30	260.00	252	3	Right
35	Cereal Bars	10049	L	M	0.29	51.03	84	3	Right
36	Oatmeal	3627	L	L	0.14	48.72	56	3	Right
37	Filter	628	L	L	0.02	10.19	7	3	Right
38	Tea Leaves	1739	L	L	0.01	27.95	14	3	Right
39	Nuts	7631	M	H	0.47	79.71	133	4	Right
40	Air fresheners	2834	M	H	0.46	32.48	21	4	Right
41	Pretzels/Chips	6426	L	H	0.49	41.24	133	4	Right
42	Popcorn	3757	L	H	0.50	132.76	56	4	Right
43	Cleaning Wipes	5555	M	M	0.28	80.66	56	1	Left
44	Seeds	74	H	L	0.10	1.39	14	1	Left
45	Dish Soap	4012	M	L	0.11	41.46	28	1	Left
46	Vinegar	1119	L	L	0.11	21.21	7	1	Left
47	Toilet Paper	5614	L	L	0.07	110.49	168	1	Left
48	Juice	12328	L	M	0.23	74.16	56	1	Left
49	Rice Snacks	1188	L	L	0.06	36.37	14	1	Left
50	Lotion	2187	H	M	0.32	45.63	56	2	Left
51	Insect Repellent	47	M	M	0.27	7.89	7	2	Left

52	Hardware	262	M	M	0.23	195.93	224	2	Left
53	Cat Supplies	1224	M	L	0.06	97.62	126	2	Left
54	Stain Remover	1423	M	L	0.05	35.74	21	2	Left
55	Laundry Soap	4793	M	L	0.05	109.79	126	2	Left
56	Plastic Utensils	687	L	L	0.12	2.03	7	2	Left
57	Napkins	1956	L	L	0.08	50.62	56	2	Left
58	Cups	291	M	L	0.01	14.59	7	2	Left
59	Dyer Sheets	1723	L	L	0.01	38.68	56	2	Left
60	Pet Food	3641	M	M	0.34	22.95	56	3	Left
61	Meal Replacements	713	H	L	0.14	21.91	7	3	Left
62	Dog Supplies	541	L	M	0.30	25.39	21	3	Left
63	Deodorant	3009	L	M	0.26	34.44	56	3	Left
64	Cat Food	9615	M	L	0.12	66.22	77	3	Left
65	Shaving Gel	1626	M	L	0.06	25.85	14	3	Left
66	Diapers	1153	L	L	0.10	176.13	196	3	Left
67	Baby Supplies	571	L	L	0.10	8.52	7	3	Left
68	Shampoo	320	M	L	0.05	10.23	21	3	Left
69	Dog Food	1426	M	L	0.04	113.06	168	3	Left
70	Hair Supplies	283	L	L	0.03	7.11	7	3	Left
71	Soap	6404	L	L	0.07	72.27	56	3	Left
72	Nutrition Bars	1204	H	M	0.28	21.45	14	4	Left
73	Vitamins	1938	H	M	0.26	17.06	14	4	Left
74	Toothpaste	7025	H	L	0.07	68.18	63	4	Left
75	Drugs	1192	H	L	0.07	15.58	14	4	Left
76	Eye Care	604	H	L	0.07	11.31	7	4	Left
77	Ointments	1462	M	L	0.09	25.38	21	4	Left
78	Personal Products	163	H	L	0.04	4.40	7	4	Left
79	Medicine	135	M	L	0.04	0.89	7	4	Left
80	Cough Drops	4162	H	L	0.02	27.60	21	4	Left
81	Antacid	1286	H	L	0.02	16.67	14	4	Left
82	Feminine Products	2865	L	L	0.04	131.48	105	4	Left
83	Pain Medication	2158	H	L	0.01	19.30	14	4	Left
84	Boost Drinks	639	H	L	0.01	40.60	42	4	Left

Appendix D. Comparison of Impulse Profit Estimates from our Model with Estimates in the Literature

We present an approach to evaluate how the impulse profit estimates from our model (based on our sample dataset) compare to what has been reported in the literature. First, we show the steps of computing a range of impulse profit per shopper based on values found in literature and products used in our dataset. We then compare this range to low and high estimates from our experiments using a {90°,0°} layout as a baseline. Finally, we contextualize the potential improvements in marginal impulse profit from varying θ and α from a {90°, 0°} layout.

From literature, the average shopper basket size at a typical grocery store ranges from \$40 - \$60 (Stilley et al., 2010; Hui et al., 2013). We multiply each of these values by low and high estimates of impulse revenue as a % of total revenue; we use ±10% of the average values found in the literature (Hui et al., 2013). These result in an estimated impulse revenue of \$12 - \$30 (see Table D1). To then estimate impulse profit (the focus of our study), we first sort the profit margin among the actual products we had access to from a retailer and compute the 1st and 3rd quantiles (20% and 40%, see table). Multiplying these by our estimated impulse revenue range results in an estimated impulse profit of \$2.40 - \$12.00 per shopper.

Next, we derive the impulse profit per shopper resulting from our model. For this, we consider a baseline layout of (90°, 0°) racks, using the Demand Ordering Rule and Impulse Ordering Rule (both using the Distance Location Rule) as our low and high estimates respectively. Table 6 in the manuscript provides the objective value (marginal profit, after discounting for space). We add the cost of floor space back to this objective value to derive the underlying impulse profit per shopper.

However, we must also consider that our layout represents only a section of a store. The product categories used in our experiments is a subset (see Appendix C) of the complete list of product categories obtained from a Midwest retailer. The number of allocations assigned to each product category is taken straight from this dataset, in addition to the height and width of each facing on the shelf. Thus, we can calculate the allocated shelf area, and then derive the number of 1x1 ft locations assigned to each product category (we round to the nearest 7 to create whole columns). That is, the product categories used in our experiments were pre-derived to fill a 6-rack layout (3 racks on each side of the main shopper pathway), each with a perimeter of 110ft and a height of 7ft. Based on the allocated area for all product categories found in the *complete* dataset, the shelf space of product categories used in our experiments constitutes approximately 50%. The complete list of product categories from the Midwest retailer, however, did not include "fresh" items usually found in grocery stores, such as fruit, produce, deli, and bakery; alcoholic beverages were also excluded. Given this, we estimate that our 6-rack layout makes up approximately 30%-40% of the total product shelf space (for our Midwest Retailer).

Therefore, we scale our estimated impulse profit per shopper. Table D1 shows that the range for impulse profit per shopper derived from the literature (\$2.40 - \$12.00) is smaller than, but still overlapping the range produced by our model (\$6.05 - \$28.87). One likely explanation for this discrepancy, more particular with the high estimate, is that our experiments assumed the impulse ordering rule, which placed the product categories with highest impulse potential (unit profit * impulse purchase rate) in the most visible locations. In reality however, product groups are often located in aisles based on affinity and/or attributes (e.g., medicine, cough drops, and antacid product groups would likely be placed next to each other, as opposed to perhaps vitamins being located in between these groups). In other words, it is unlikely a true impulse ordering rule is used in in a real store; thus, justification for the upper values in the ranges being a bit high in our case.

Now considering the best improvements we generated over our baseline layout (i.e., cases 3 and 4 in Table 6), we show the impulse profits per shopper for {23.3°, 0°} and {27.4°, 60.5°} layouts (cases 5 and 6), which equate to improvements of 243% and 58%, respectively. While on the surface the improvement of 243% seems too high to be realistic, we reiterate our discussion from the paper, which argues that the Demand Ordering Rule in combination with a {90°,0°} layouts essentially hides a majority of the products with high impulse potential from the shopper; varying the layout to expose these products to shoppers passing by dramatically increases the expected impulse profit. That being said, as brought up earlier, grocery stores usually do not order products solely on demand, nor impulse potential; there usually is some middle ground (i.e., product affinity). Thus, the 243% increase can be seen as an upper bound on the impulse revenue increase.

Table D1. Steps for deriving impulse profit per shopper.

Case	Basket Size	% of Revenue as Impulse	Impulse Basket Size	% of Revenue as Profit	Impulse Profit Per Shopper	
1	$ 40.00	30%	$ 12.00	20%	$ 2.40	From Literature
2	$ 60.00	50%	$ 30.00	40%	$ 12.00	
			Impulse Profit Per Shopper (Store Section)	% of Store	Impulse Profit Per Shopper (Whole Store)	
3	Demand Ordering Rule	Baseline (90°,0°)	$ 2.42	**40%**	**$ 6.05**	Our Model
4	Impulse Ordering Rule	Baseline (90°,0°)	$ 8.66	**30%**	**$ 28.87**	
5	Demand Ordering Rule	Best (23.3°, 0°)	$ 8.30	**40%**	**$ 20.75 (+243%)**	
6	Impulse Ordering Rule	Best (27.4°, 60.5°)	$ 13.67	**30%**	**$ 45.57 (+58%)**	